Electrochimica Acta 202 (2016) 316–324

Contents lists available at ScienceDirect

Electrochimica Acta

journal homepage: www.elsevier.com/locate/electacta

Testing phosphate ions as corrosion inhibitors for construction steel in mortars

L. Yohai, M.B. Valcarce[1], M. Vázquez[1,*]

División Electroquímica y Corrosión, Facultad de Ingeniería, INTEMA, UNMdP-CONICET, J. B. Justo 4302, (B7608FDQ) Mar del Plata, Argentina

ARTICLE INFO

Article history:
Received 18 June 2015
Received in revised form 16 December 2015
Accepted 19 December 2015
Available online 22 December 2015

Keywords:
mortars
corrosion inhibition
phosphate ions
chloride

ABSTRACT

The purpose of this investigation is to analyze the effectiveness of phosphates as inhibiting agents for steel bars embedded in mortars. Three mix designs were selected for this study: mix A had no admixed chlorides and was used as reference; mix designs B and C were contaminated with 1% in weight of chlorides/weight of cement and mix C also incorporated 7% $Na_3PO_4.12\,H_2O$. After setting for 48 h, the samples were cured for 7 days immersed in water. Three specimens of each group were then immersed in aerated saline solutions 0.5 mol L^{-1} NaCl during 720 days. The corrosion potential (*Ecorr*), the polarization resistance (*Rp*) and the electrochemical impedance spectra were recorded regularly. After 720 days of immersion one set of mortars was anodically polarized and another set cathodically polarized. After that, Raman spectra of corrosion products were registered. Additional specimens were used to evaluate porosity and chloride profiles. The presence of phosphate ions as inhibitors has no effect on *Ecorr* values and suggests mixed-type inhibition. Mix C remains passive until 180 days of exposure, with Rt> 100 kΩ cm^2. At longer times, Rt decreases in time but the inhibition percentage is always higher than 95% when evaluated by impedance spectra. Using *Rp*, inhibition stays above 70%. Anodic and cathodic polarization curves, together with corrosion potential values, suggest that phosphates behave as a mixed-type inhibitor.

1. Introduction

Reinforced concrete is one of the most widely used structural materials in the construction industry worldwide. However, faulty concrete formulations or an aggressive service environment promote premature deterioration and failure. Among the most frequent problems, reinforcing steel bar (rebar) corrosion is at the top of the list.

Concrete, and the pore solution in contact with steel, provide a highly alkaline environment which helps to develop a passive layer that protects the rebar from active corrosion [1]. There are many factors that influence the stability of the passive film such as the chloride ions content in concrete [2–4] and concrete carbonation [5–7], the mix design and curing conditions of concrete, the chemical composition of the pore solution and the thickness of the concrete cover [8,9].

Many local variables, including the mineralogy of raw materials, the exposure conditions and traditional construction practices, may also influence rebar corrosion. For example, since the early seventies, the use of sea sand for civil construction in certain cities located at the coastal region of Argentina has become quite common. As a consequence, there are many structures nowadays presenting severe damage caused by rebar corrosion [10].

Various procedures are frequently employed in an attempt to minimize rebar corrosion, such as cathodic protection [11], realkalinization [12], and the application of coatings to the external concrete surface or to the reinforcing steel bars [13–15]. Another alternative is the use of inhibitors, which can be cost-effective and are easy to apply. They can be used in reinforced concrete by adding the inhibiting agent to the mixing water during the concrete preparation or by applying it to the external surface of hardened concrete. Reviews of the most commonly used corrosion inhibitor types in concrete repair systems and the various possible mechanisms of inhibition are available [16–18]. The most commonly admixed inhibitors are formulated on the basis of nitrite ions [19,20]. However, nitrites should be used with care when lixiviation can contaminate surrounding soil or water.

Other ions have been investigated as candidates to inhibit pitting corrosion of steel, namely chromates, phosphates,

* Corresponding author at: División Electroquímica y Corrosión, Facultad de Ingeniería, Universidad Nacional de Mar del Plata, INTEMA, CONICET. Juan B. Justo 4302 – B7608FDQ Mar del Plata – Argentina. Tel.: +54 223 481 6600 ext 244; Fax: +54 223 481 0046.
E-mail address: mvazquez@fi.mdp.edu.ar (M. Vázquez).
[1] ISE member.

http://dx.doi.org/10.1016/j.electacta.2015.12.124
0013-4686/

tungstates and molybdates [21–23]. Phosphates present some interesting advantages such as low cost and low toxicity.

To evaluate the efficiency of phosphate ions as inhibitors for reinforced concrete application, some authors simulate pore solutions [24–30]. In contrast, few articles have reported evaluations of the phosphate ions effectiveness in mortars or cement paste at long exposure times [31,32]. The interaction between phosphate ions with cement paste is complex. Some authors argue that phosphates can alter the mechanical properties of concrete or modify curing times, as they decompose and precipitate as calcium phosphate, in turn decreasing the efficiency of the inhibitor [33,34]. However, other authors claim that this inhibitor does not interfere and demonstrate that it is effective in mortars [31,32,35]. Besides, the adequate phosphate to chloride ratio in mortars is controversial and the inhibition mechanism is not clear. Some authors propose a dual effect, where calcium phosphate could block the pores avoiding diffusion of aggressive species while iron phosphate could block cathodic or anodic sites [31,32,36,37].

Our previous work focused on phosphate ions as inhibitors for highly alkaline pore solution contaminated with chlorides. A mixed-type corrosion mechanism was found when phosphate to chloride ratio is 1 [29]. That study in simulating pore solutions is being extended to carbonated solution and is currently in press [38].

In parallel, the purpose of this investigation addresses the effectiveness of phosphates as inhibiting agents but now for steel bars embedded in mortars after long exposure times. Papers published earlier by other authors, that address the effect of phosphates in mortar, are either accelerated tests [36], deal with short term exposures [26,37], use monofluorphosphates [35], or study pre-oxidized or as-received rebars [32].

2. Experimental

2.1. Samples design

The study was performed using cylindrical mortar test specimens (2.8 cm in diameter by 8 cm high) containing one rebar segment and leaving a 1 cm mortar cover (see Fig. 1). The rebar segments presented an exposed area of 12.6 cm^2. Table 1 presents the chemical composition of the reinforcing steel bars used in the study. The bars were abraded with 1000 grade emery paper just before embedding them in the mortar paste.

Table 1
Chemical composition of the steel rebars.

% (w/w)	Mn	C	Si	Cu	impurities
	0.63	0.30	0.26	0.23	0.24

Portland cement was used with water to cement ratio of 0.6 and sand to cement ratio of 3 (ASTM C-305). Three mix designs were selected for this study. Mix **A** had no admixed chlorides and was used as reference. Mix designs **B** and **C** reproduced the case of reinforced concrete structures heavily contaminated with a known amount of chlorides (1%, expressed in weight of chlorides/weight of cement). Mix **C** also incorporated 7% $Na_3PO_4.12H_2O$, where the phosphate to chloride ratio is 0.6. The mortars were prepared using river sand and Portland cement containing less than 0.1% per weight of chloride ions.

After setting for 48 h, the samples were cured for 7 days immersed in water. Three specimens of each group were then immersed in aerated 0.5 mol/L NaCl solutions (equivalent to 2.92% w/V).

Additional specimens with the same composition but without rebars were casted in parallel. These were used to evaluate physical properties, as described below. The size of these samples is the same as those described above.

2.2. Electrical and electrochemical measurements

Typical electrochemical parameters normally used to characterize the corrosion behavior of reinforcing steel in concrete were monitored periodically during 720 days. These included the corrosion potential (*Ecorr*), the polarization resistance (*Rp*) and polarization curves. Also, the electrochemical impedance spectra were recorded regularly. All these tests were carried out with the mortars immersed in 0.5 mol/L NaCl solutions.

The corrosion potential was measured against a mercury/mercuric oxide reference electrode, Hg/HgO in KOH 1 mol/L (E = 0.123 V vs. NHE) using a Gamry Reference 600. The reference electrode was positioned inside a Luggin capillar, with the tip touching the mortar external surface. The counter electrode was a platinum wire of large area.

Using the same set-up, polarization resistance (Rp) was evaluated as $\Delta V/\Delta i$, from potential sweeps up to ± 0.015 V from *Ecorr* at a scan rate of 10^{-4} V s^{-1}. The results were corrected so as to

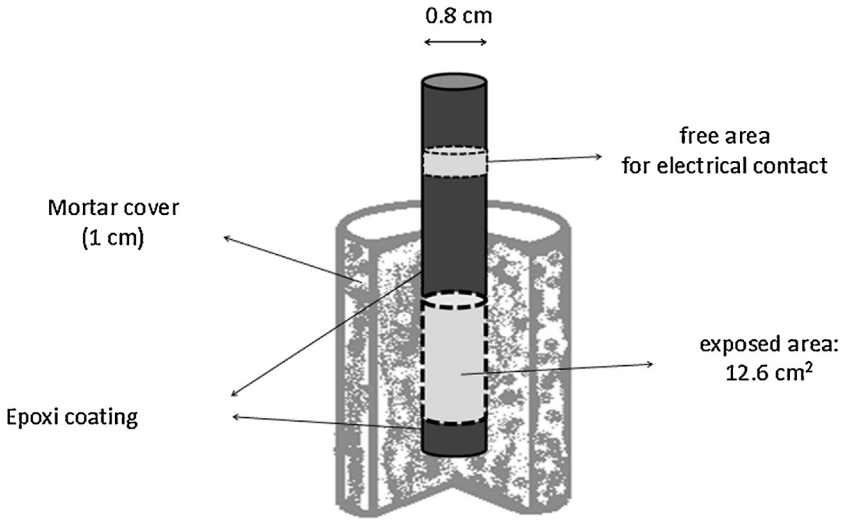

Fig. 1. Cylindrical mortar test specimens including one rebar segment.

take into account the high resistivity of mortars by subtracting the mortar resistance calculated by EIS.

For the anodic polarization curves, the potentiodynamic scan started at *Ecorr*. The scan direction was reversed when reaching 1 mA cm^{-2}. Similarly, for the cathodic polarization curves, the potentiodynamic scan started at *Ecorr* and stopped at -1.1 V. The potential was swept at 10^{-4} V s^{-1}. Anodic and cathodic polarization curves were performed after 720 days of exposure, just before the samples were destroyed for visual inspection.

Electrochemical impedance spectroscopy (EIS) tests were performed at open circuit potential, without stirring or deaereating. The amplitude of the AC applied potential signal was ± 0.01 V_{rms} while the frequency varied between 20 kHz and 1 mHz. The results were analyzed using two different equivalent circuits presented in Fig. 2. The experimental data were fitted to the proposed equivalent circuit using ZView™ [39].

2.3. Ex-situ Raman spectra

The Raman measurements were carried out using an Invia Reflex confocal Raman microprobe with Ar^+ laser of 514 nm in backscattering mode, with a laser spot diameter of 10 μm. An exposure time of 50 s and 3 accumulations were used, with a 50 X objective. The laser power was 25 mW. The effect of the laser heating on the corrosion products was evaluated before the final spectra were recorded. The laser power was increased progressively on different zones, until the power with the optimal noise/signal ratio was found, without observing any changes in the composition. Raman spectra were collected on at least five representative spots, either on steel or on mortar, after having subjected the electrodes to anodic polarization curves.

2.4. Physical characterization of the mortars

2.4.1. Porosity

Porosity was evaluated as specified in standard ASTM C-642. The weight of mortar samples was registered in three different conditions: samples dried in an oven at 105 °C (P_A), after immersion in water for 24 h and boiled for 6 h (P_B), and weighting the immersed sample suspended in water (P_C). Then, porosity can be calculated using Eq. (1). Three independent values were measured and averaged.

$$P\% = \frac{P_B - P_A}{P_B - P_C} x100 \quad (1)$$

2.4.2. Chloride profiles

Mortar samples without rebars were immersed in NaCl 0.5 mol L^{-1} during 360 days. These samples were prepared with mix A and all the external surface but one of the flat extremes was coated with epoxy resin. At the end of the exposure time the sample was dried and cut into 1 cm width rods. In each rod, the total chloride ions concentration was determined by titration following the recommendation in ASTM C-1152.

In order to analyze the chloride transport mechanism within the specimens, the effective diffusion coefficient (D_C) was determined by solving Fick's second law expressed as,

$$\frac{\partial C}{\partial t} = D_C \frac{\partial^2 C}{\partial x^2} \quad (2)$$

where C is the total chloride concentration, x is the distance and t is the time.

3. Results and discussion

3.1. Evolution of the corrosion potential

Fig. 3 presents the evolution of the corrosion potential over the 720 days of exposure (average of three independent values). The values present a clear tendency that becomes evident after the first 100 days of exposure. As expected, when the mortar samples are immersed in the saline solution, *Ecorr* attains values typical of steel in active corrosion. The presence of phosphate ions as inhibitors has no effect on *Ecorr* values in agreement with results reported by other authors [31,32]. In simulated pore solutions, it had been observed before that phosphate ions may act as a mixed inhibitor [29], so *Ecorr* cannot be used as a sole criterion for inhibiting efficiency.

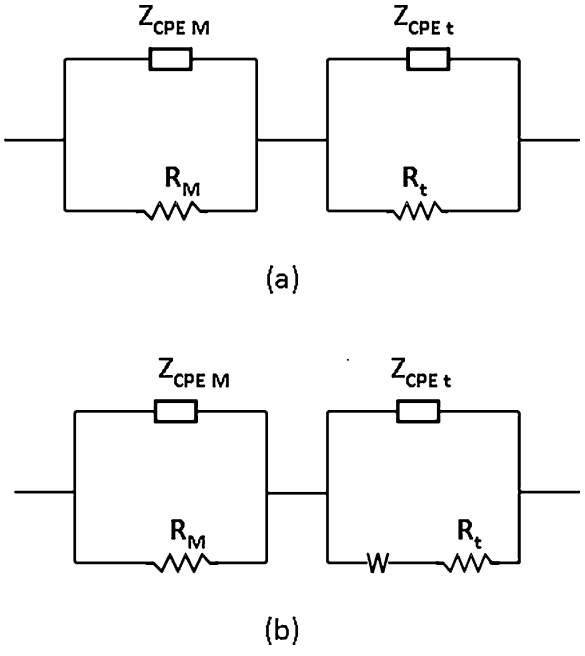

Fig. 2. Equivalent circuits used to analyze the results. Circuit (a) was used to fit the results for the first 30 days of exposure of mixes **A** and **B** and the first 180 days of exposure for mix **C**. Circuit (b) was used after these periods of time.

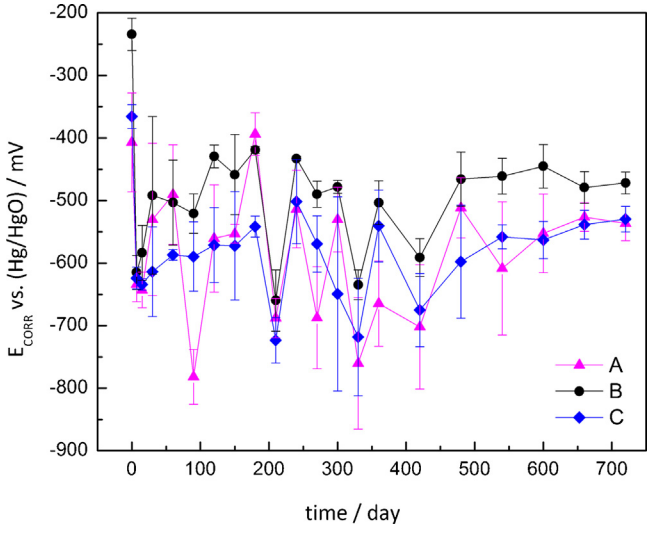

Fig. 3. Evolution of the corrosion potential over exposure time. Error bars illustrate the dispersion from at least 3 independent measurements.

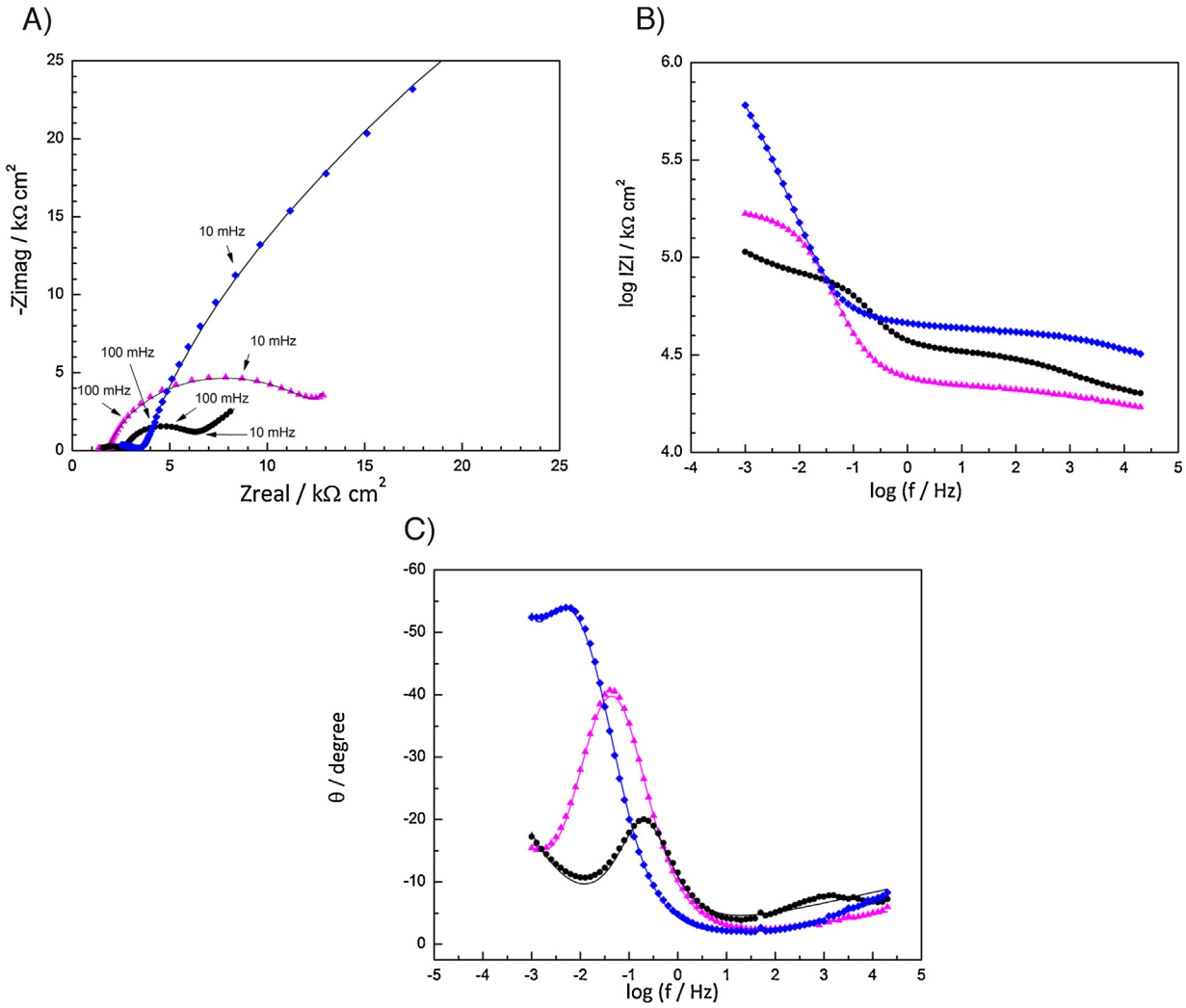

Fig. 4. Impedance spectra for mix designs **A**,**B** and **C**, registered after 720 days of exposure. Mix A (—▲—); Mix B (—●—) and Mix C (—♦—). Points represent the experimental data and lines show the fitting results.

3.2. Electrochemical Impedance Spectroscopy

The impedance spectra registered for mix designs A, B and C after 720 days of exposure, together with the fit results are shown in Fig. 4a–c in the form of Nyquist and Bode plots.

Surface roughness, grain boundaries and impurities can justify the use of CPEs in equivalent circuits that model corroding metals. For these elements, the impedance is frequency-dependent, and can be expressed as follows:

$$Z_{CPE} = [Q(jw)^n]^{-1} \quad (1)$$

where Q is a constant with dimensions of $\Omega^{-1}\,cm^{-2}\,s^n$ and n a constant power, with $-1 < n < 1$.

Warburg impedances and CPEs where *n* is close to 0.5 are used to model surface layers with increasing ionic conductivity due to corrosion processes inside the pores, and the associated diffusion process. If the surface layer is thin, low frequencies penetrate the entire thickness and can be represented by a finite length Warburg

Table 2
Optimized parameters fitting data in Figs. 4 a, b and c to the equivalent circuits proposed in Fig. 1.

	mix A					mix B					mix C				
Time (days)	0	180	360	540	720	0	180	360	540	720	0	180	360	540	720
R_M (kΩ cm²)	0.78	8.6	3.5	2.2	2.0	2.5	4.3	3.4	4.1	3.3	1.0	4.2	2.9	3.4	3.7
Q_M ($\mu\Omega^{-1}\,cm^{-2}\,s^n$)	0.14	33.2	101.6	25.3	35.4	0.14	39.2	54.8	56.5	40.5	0.10	1.73	17	10.8	6.5
n_M	0.52	0.12	0.11	0.16	0.19	0.21	0.15	0.15	0.15	0.18	0.36	0.32	0.21	0.23	0.26
W_R (kΩ cm²)	–	15.6	8.5	5.8	9.6	–	13.9	7.3	11.5	11.6	–	–	136	215	122
T (s)	–	752	674	683	1308	–	735	1023	1430	1579	–	–	661	1146	588
n_W	–	0.71	0.77	0.75	0.50	–	0.56	0.59	0.53	0.53	–	–	0.57	0.75	0.67
Q_t ($\mu\Omega^{-1}\,cm^{-2}\,s^n$)	55.8	136	769	1126	705	30.2	253	416	293	376	38.9	121	660	939	937
n_t	0.86	0.90	0.83	0.82	0.87	0.87	0.83	0.91	0.95	0.95	0.88	0.80	0.75	0.81	0.83
R_t (kΩ cm²)	835	39.1	10.2	9.5	10.1	1413	2.7	2.2	3.3	2.9	1499	213	95.8	62.3	70.5
η%											5.7	96.6	97.7	94.7	95.9

element (Eq. (2)):

$$Zw = \frac{W_R}{(iTw)^n}\tanh(iTw)^n \quad (2)$$

where W_R describes solid phase diffusion and T can be associated to the effective diffusion coefficient (D) and the effective diffusion thickness (L) by $T = L^2/D$ [38].

The experimental data can be reasonably fitted to the equivalent circuits proposed in Fig. 2. The fitting parameters are presented in Table 2. In Fig. 2a and b, R_M and Q_M represent the mortar resistance and the mortar pseudo-capacitance, respectively. Q_t is the passive layer pseudo-capacitance and R_t charge-transfer resistance for metal dissolution. The circuit in 2a has been used before for passive steel in mortars [32,40]. The circuit in 2b includes a Warburg element associated to finite length diffusion that could be related to diffusion through a finite rust layer [32,41].

The circuit in Fig. 2a was used to fit the results for the first 30 days of exposure of mixes **A** and **B** and until 180 days of exposure for mix **C**. The other results in Table 2 were calculated fitting with the circuit in Fig. 2b. At long exposure times, corrosion products may accumulate, justifying the need to include elements that represent diffusion processes. The percentage of inhibition presented in Table 2 was calculated as

$$\text{Inhibitor } \% = [1\text{-}(R_t \text{ without inhibitor}/R_t \text{ with inhibitor})] \times 100 \quad (3)$$

taking the results from mix **B** as reference.

The first time constant does not show significant differences for the three mixes. This can be expected, as this term is associated to mortar properties.

After 180 days of immersion, mixes **A** and **B** show $R_t \leq 10\ k\Omega\ cm^2$, as expected for cases where steel is in active dissolution [42]. Instead, for mix **C**, R_t is always greater than 100 $k\Omega\ cm^2$ during the first 180 days, suggesting that steel remains in the passive state [2,42]. This was confirmed by visual inspection: only specimens prepared with mortars **A** and **B** presented cracks on the surface. For longer times of exposure, R_t decreases slightly but is always one order of magnitude higher for mix **C** than for mixes **A** and **B**. It has been suggested that after extended immersions in chloride-rich media, chloride concentration can surpass phosphates concentrations, leading to a decrease in the inhibition efficiency [32]. Even if that were the case, it has to be stressed that the inhibition percentage stays close to 95% during the whole second year of immersion.

The accumulation of corrosion products can be analyzed in terms of the Warburg element in circuit 2b. The resistive component W_R is 10 times higher for mix **C**, as a result of the presence of phosphates as inhibiting agent. Also, the diffusion term T is lower, which together with a higher W_R suggest the presence of a thin and compact layer of corrosion products. As regards the CPE, it can be seen that Q_t values increase with immersion time. However, n_t remains close to 1, indicative of a capacitive behavior. It would be expected that the increment in Q_t was accompanied by a decrease in n_t with the immersion time. Yet, Q_t is the result of a combination of different processes occurring on the metal surface: activation and/or mass transfer control, the presence of a passive film, and even localized attack. Also redox processes taking place within the oxide layer should probably be taken into account. This is why it is difficult to propose a physical interpretation of this behavior.

The appearance of the samples is in agreement with these results, as can be seen in Fig. 5. Mixes **A** and **B** presented cracks before the year. Due to the accumulation of corrosion products during the active degradation of the steel bar, mechanical stresses generate fractures in the mortars. These allow the access of aggressive species, resulting in an even greater corrosion rate. In contrast, no cracks or corrosion products were visible on the surface of mix **C**, confirming that these samples remain passive.

3.3. Polarization resistance

Polarization resistance values (R_p) were calculated from linear sweeps, as described in Section 2.2. The values, derived from the slope of the potential vs. current graph, were corrected (R_p^*) by subtracting the mortar resistance (R_M), calculated from EIS results:

$$R_p^* = R_p - R_M \quad (4)$$

Fig. 6 shows the evolution of R_p^* in time. Polarization resistance values higher than 100 $k\Omega\ cm^{-1}$ are typical of the passive state, while values falling below 10 $k\Omega\ cm^{-1}$ are characteristic of actively corroding steel [2,42]. These values are shown with dashed lines in the graph. R_p^* values indicate that mix **A** remains passive for the first 30 days. Later, R_p^* values approach 10 $k\Omega\ cm^{-1}$, suggesting that passivation is lost. Mix design B presents a similar behavior, which indicates that chloride ions are aggressive regardless of them being incorporated to the mortar or diffusing from the electrolyte. This last situation however, will depend on the porosity of the mortar. Instead, in spite of the presence of chloride ions, R_p^* values for mortar C remain above 100 $k\Omega\ cm^{-1}$ during the first 270 days of immersion and later drop slightly below that value, remaining at around 65 $k\Omega\ cm^{-1}$ until 720 days of immersion. This different behavior results from the presence of phosphates in the mortar. Fig. 6 also shows the inhibition percentages on the right vertical axis. These were calculated from R_p^* for mix **C**, with an

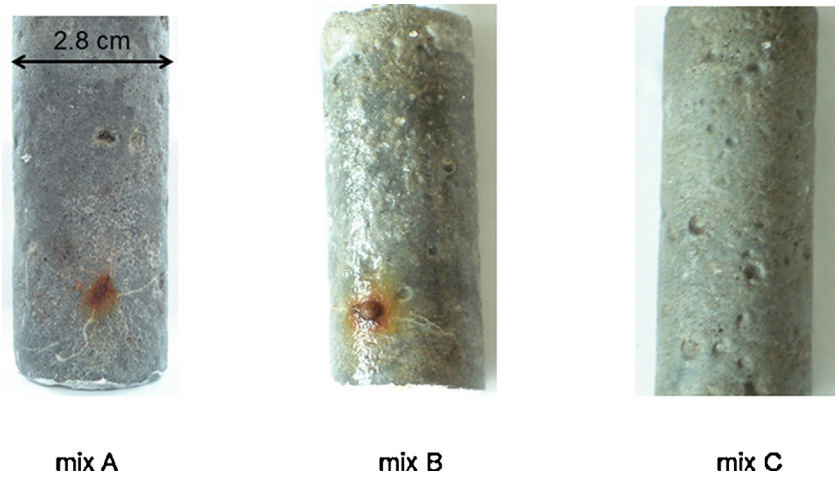

Fig. 5. Images of the mortars with rebars after 365 days of immersion.

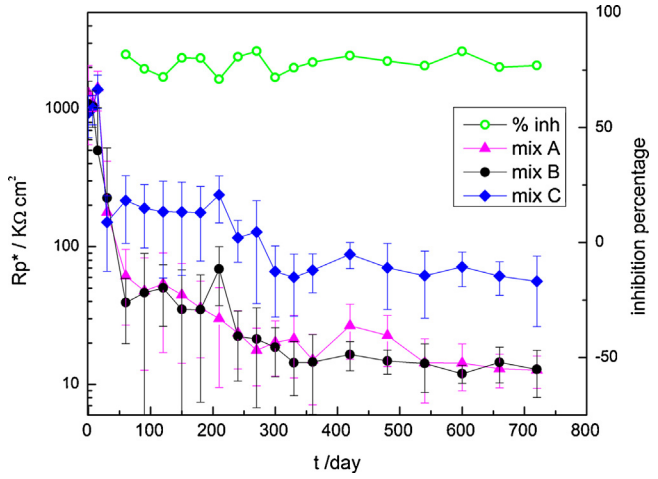

Fig. 6. Polarization resistance values (Rp) registered during 720 days of immersion in NaCl 0.5 mol L^{-1}. Mix A (—▲—); Mix B (—●—) and Mix C (—♦—). % Inhibition (—●—). Error bars illustrate the dispersion from at least 3 independent measurements.

equivalent to, and again taking mix **B** as reference (no inhibitor condition). On average, inhibition values are higher than 70% and stable in time. Even if these Eq. (3) percentages are slightly lower than those calculated from EIS and presented in Table 2, the effectiveness of phosphates as inhibiting agents is clear. Rp measurements by linear polarization were carried out using a scan rate of 0.1 mV s^{-1}. This scan rate can be converted to a frequency and corresponds to 0.0016 Hz in the EIS spectrum. The Rp* value obtained contains contributions from the diffusion terms in the cases where the equivalent circuit from Fig. 2b applies. In contrast, Rt values obtained by EIS are calculated extrapolating to very low frequencies and the diffusion contribution can be separated from the Rt values fitting with the equivalent circuit in Fig. 2b. This is the origin of the discrepancy. Even if the values are different, the tendencies observed are similar with both techniques

3.4. Polarization curves

After 720 days of immersion, the steel bars were anodically polarized. The results are shown in Fig. 7a. The curves show no evidence of passive behavior. This is to be expected since EIS results show that after 720 days of immersion the rebars present active state in every tested condition. However, within most of the potential range, the anodic current in the case of mix **C** is lower than for mixes **A** and **B**. This might suggest that the anodic process controls the global corrosion rate. The appearance of the samples after carrying out the anodic polarization curves can be seen in Fig. 7b.

Cathodic polarization curves were also recorded after 720 days of immersion, using different samples. The results are presented in Fig. 8. The curves show a mixed control zone between *Ecorr* and -0.6 V. Then there is a steady increase in the current and no limiting current can be clearly identified. However, the cathodic current in the case of mix **C** is lower than for mixes **A** and **B**, as was the case for the anodic current. When the inhibitor affects both, the anodic and the cathodic branch, mixed control can be proposed.

3.5. Raman characterization

Once the anodic and cathodic curves had been recorded, the mortars were fractured applying a static radial charge. Rebars in mix **B** (see Fig. 7b) showed the most severe degree of attack. The corrosion products were analyzed by Raman confocal spectroscopy in regions of particular interest. Fig. 9a and b show Raman confocal

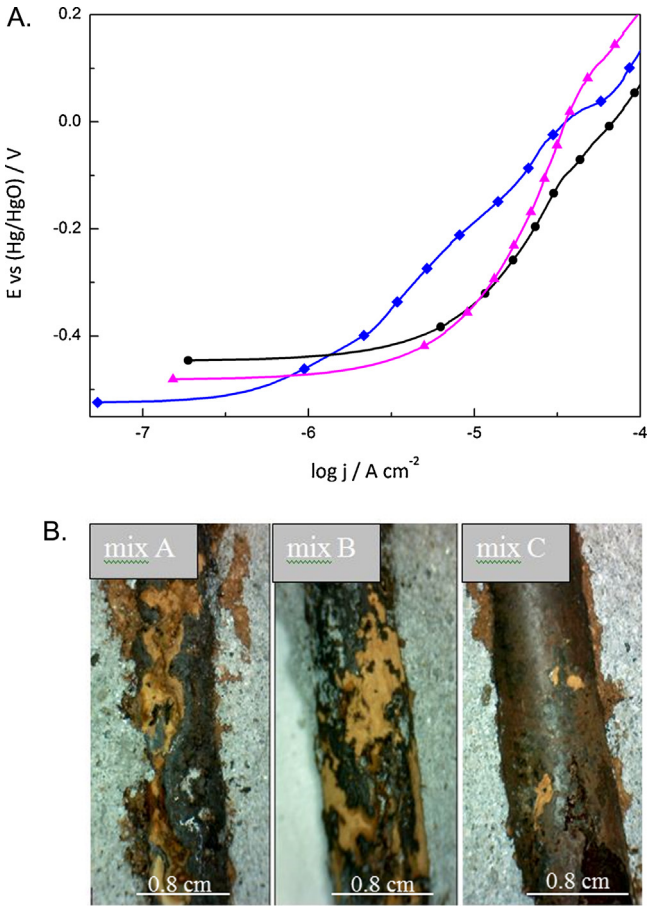

Fig. 7. a Anodic polarization curves of rebars after being 720 days under immersion in NaCl 0.5 mol L^{-1}. Mix A (—▲—); Mix B (—●—) and Mix C (—♦—). Lines represent the experimental data and points are shown to distinguish the curves. b Photographs of the rebars after anodic polarization.

spectra for two zones of steel in mortars B and C, after the cathodic polarization curve had been recorded. The composition of the mortar was also evaluated in a third zone. The signal from the reddish corrosion products is stronger in the absence of phosphates (mix B). In this region, α-FeOOH and/or α-Fe_2O_3 (at 220 cm^{-1}, 280 cm^{-1}, 395 cm^{-1}, 484 $cm^{-1}$and 595 cm^{-1}) can be

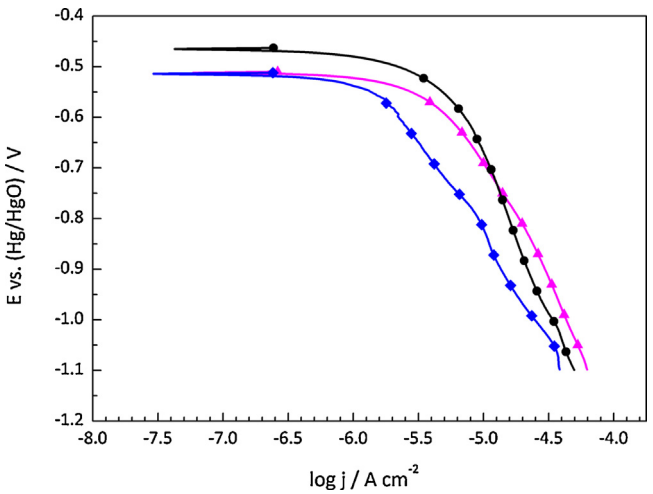

Fig. 8. Cathodic polarization curves of rebars after 720 days of immersion in NaCl 0.5 mol L^{-1}.Mix A (—▲—); Mix B (—●—) and Mix C (—♦—). Lines represent the experimental data and points are shown to distinguish the curves.

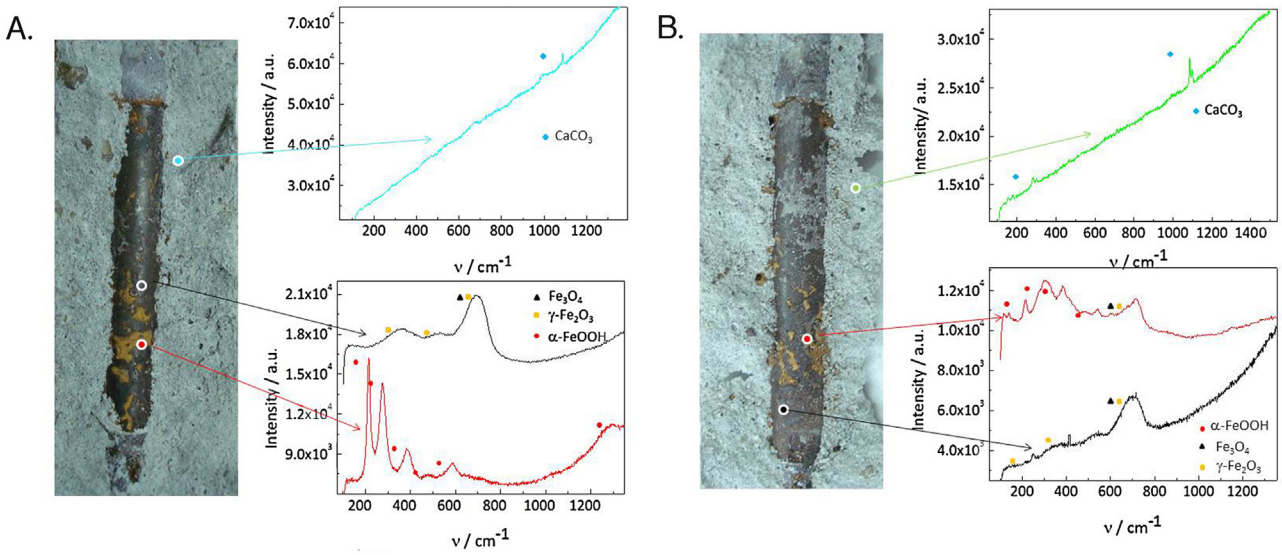

Fig. 9. a Raman spectra of corrosion products and mortar after cathodic polarization curve for the chloride contaminated mortar (mix **B**). b Raman spectra of corrosion products and mortar after cathodic polarization curve for the mortar containing chloride and phosphate ions (mix **C**).

identified. The darker corrosion products show evidence of the presence of magnetite Fe_3O_4 (at 680 cm^{-1}) and maghemite, γ-Fe_2O_3, (at 360 cm^{-1}, 500 cm^{-1} and 710 cm^{-1}). The position of the peaks is similar for both mortars although the relative intensities are different. In the case of mix **C**, no evidence of the phosphate signal was found, either on the rebar surface or in the mortar. Only $CaCO_3$ could be identified in the spectra recorded on the mortar, both in mixes **B** and **C**. This is in agreement with a similar result reported by Dhouibi [31], who detected the presence of phosphates only until 30 days of immersion. In the IR spectra they observe that phosphates acidify concrete and interfere in the equilibrium CO_3^{-2}/HCO_3^-, facilitating the precipitation of crystalline $CaCO_3$. In contrast, Shi and Sun [32] explained the decay in phosphates inhibition efficiency as due to the precipitation of $Ca_3(PO_4)_2$. In turn, $Ca_3(PO_4)_2$ could produce a delay in the diffusion of detrimental substances [32,36].

The absence of a band related to phosphate ions in the spectrum could be associated to a very low sensibility of the technique. Various factors could explain a weak signal, such as poor backscattering, products with a low crystalline degree, a porous and inhomogeneous surface and restricted vibrational modes affected by the chemical environment. In addition, the phosphate ions signal coming from the corrosion products formed after long immersion times could be diluted by the majority presence of iron oxides in the surface layer. To verify these assumptions, Raman spectra were recorded on mortars prepared with mix C that were exposed to the laboratory atmosphere (never immersed in any electrolyte) where phosphate ions are undoubtedly present. After two years, no phosphate ions could be detected by Raman spectroscopy.

3.6. Porosity

Porosity was evaluated as described in Section 2.4.1. The average value was 17.6 ± 0.6%, which is in good agreement with the sand/cement and water/cement ratios employed to prepare these mortars. This value would correspond to a standard quality concrete.

3.7. Chloride diffusion

Fig. 10 shows the profile in chloride concentration after 360 days of immersion in 0.5 mol L^{-1} NaCl. The dotted lines represent the limits between low (0.2–0.4), moderate (0.4–1.0) and high (>1) corrosion risk. For the first 4 cm, the chloride content exceeds the critical concentration of 1% that triggers steel corrosion. As shown in Fig. 1, the rebar was positioned at 1 cm from the external surface, well within the high risk zone. Diffusion is a complex process that involves chemical and physical aspects. However in most cases, it can be analyzed using Fick's laws, as described in Section 2.4.2 and Eq. (2) [43]. While using this equation, one assumes that chloride ions move driven by a concentration gradient and that the diffusion coefficient is constant in time and space. Also, the chloride surface concentration (*Cs*) was assumed to remain constant in time for the immersed specimens. The analytical solution is shown in Eq. (4) in terms of the error function (erf):

$$C_t = C_S\left[1 - erf\left(\frac{x}{2\sqrt{D_C t}}\right)\right] \quad (4)$$

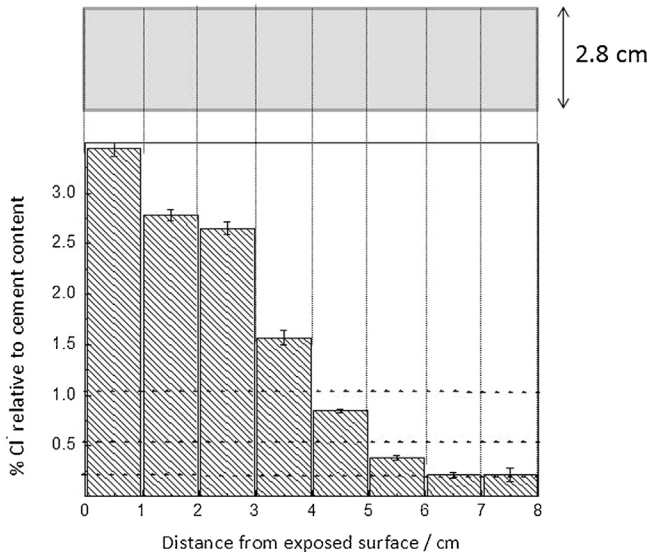

Fig. 10. Chloride concentration profiles obtained from the chloride-free mortar (mix A) after one year of exposure to NaCl 0.5 mol L^{-1}.

where x represents the depth in the mortar, Ct the chloride concentration at x in%, Cs the chloride concentration at the surface in%, t the exposure time in seconds and D_C is the diffusion coefficient. C_t was evaluated at various x values after 1 year of immersion. By fitting the experimental data to eqn. 4, Cs was found to be 4.06% in weight of cement and D_c could be calculated as $2.38 \times 10^{-7}\,cm^2\,s^{-1}$. This value is in good agreement with those reported in the literature for mortars with water/cement ratios of 0.6 [3,44].

3.8. Inhibition by phosphate ions

Various papers [24–30] deal with the effect of phosphate ions in pore solutions that simulate concrete. In these conditions it is possible to propose an inhibition mechanism without taking into account the interaction between phosphate ions and cement. However, these results must be complemented with mortars testing because it has been argued that the interaction of phosphate ions with the cement paste can be detrimental to the efficiency of phosphate ions as corrosion inhibitors.

In a previous work [29] a detailed study of the effect of phosphate ions as corrosion inhibitors on steel was carried out in simulated pore concrete solution (pH = 13 contaminated with chloride ions). Two solutions were used representing the chemistry of mixes with and without phosphate, similar to the mortars used in the present work. In these highly alkaline solutions, phosphate ions behaved as mixed inhibitors: there is no variation in the E_{corr} and there are pronounced changes in the anodic behavior, with no pitting attack after 90 days of immersion.

The main aspects of the mechanism that we postulated in that work are still valid in mortars: phosphate ions promote the formation of a surface layer that inhibits iron dissolution and delays oxygen diffusion.

When rebars are embedded in chloride contaminated mixes (mixes A and B), the surface layer formed at E_{corr} is composed by Fe_3O_4, γ Fe_2O_3 and FeOOH, as confirmed by Raman analysis. When phosphates are incorporated (mix C), the first step in the surface layer formation could be related to the precipitation of a thin layer of ferrous phosphate at short exposure times:

$$3Fe + 2\ PO_4^{-3} \rightarrow (Fe)_3(PO_4)_2 + 6\ e^- \quad (5)$$

Underneath this thin ferrous phosphate layer, a protective passive film of Fe_3O_4 could be formed via solid-state process. At longer times, the inner layer may grow until a black layer of corrosion products composed principally by Fe_3O_4, is observed. This can be seen by the relative intensities of the Raman signals in Fig. 9a and b and by the predominance of the black oxides after 720 days of immersion when phosphate ions are present (see also Fig. 7b). Fe_3O_4 is a good conductor; it is quite insoluble and known to inhibit iron dissolution. In addition, this layer could delay oxygen and chloride diffusion, justifying the inclusion of a Warburg element in the impedance analysis.

In agreement with previous work [32,36,37], phosphates could also combine with the Ca^{2+} ions present in the pore solution, precipitate as calcium phosphate and contribute in hindering oxygen and chloride diffusion.

5. Conclusions

The effectiveness of phosphate ions as inhibiting agents for the corrosion of rebars in mortars and the effect of chloride ions were investigated over an immersion period of two years in solutions containing 0.5 mol L^{-1} of NaCl. Samples with and without chloride and with chloride and phosphates admixed, were compared.

As expected, chloride ions are very aggressive and trigger the rebar corrosion. After 180 days of immersion there is no difference in the response of mortars with and without admixed chlorides. A relatively high porosity (17%) and high diffusion coefficient contribute to this result.

The addition of phosphates is beneficial, even in chloride-contaminated mortars. For mix C, the polarization resistance remains higher than $100\,k\Omega\,cm^2$ during the first 270 days of immersion, suggesting that the steel remains passive. This value decreases over the next 540 days, but the inhibition efficiency stays always above 95% if measured by EIS and above 70% if measured by linear polarization.

Anodic and cathodic polarization curves show that phosphates influence both processes. This, together with corrosion potential values, suggests that phosphates behave as a mixed-type inhibitor.

The presence of phosphate ions could promote the formation of a more compact and thin corrosion products layer, predominantly composed of Fe_3O_4, which inhibits iron dissolution and delays oxygen diffusion. Also, the presence of $Ca_3(PO_4)_2$ blocking pores could delay the diffusion of detrimental species.

Acknowledgments

This work has been supported by the University of Mar del Plata (Grant 15/G391), as well as by the National Research Council (CONICET, PIP0670). L. Yohai wishes to thank CONICET, Argentina, for her fellowship.

References

[1] K. Tuuti, Corrosion of Steel in Concrete, Sweedish Cement and Concrete Research Institute, 1982.
[2] M.F. Montemor, A.M.P. Simoes, M.G.S. Ferreira, Chloride-induced corrosion on reinforcing steel: From the fundamentals to the monitoring techniques, Cement and Concrete Composites 25 (2003) 491–502.
[3] X. Shi, N. Xie, K. Fortune, J. Gong, Durability of steel reinforced concrete in chloride environments: An overview, Construction and Building Materials 30 (2012) 125–138.
[4] W. Morris, A. Vico, M. Vázquez, Chloride induced corrosion of reinforcing steel evaluated by concrete resistivity measurements, Electrochimica Acta 49 (2004) 4447–4453.
[5] M. Moreno, W. Morris, M.G. Alvarez, G.S. Duffo, Corrosion of reinforcing steel in simulated concrete pore solutions effect of carbonation and chloride content, Corrosion Science 46 (2004) 2681.
[6] M.B. Valcarce, M. Vázquez, Carbon steel passivity examined in solutions with a low degree of carbonation: The effect of chloride and nitrite ions, Materials Chemistry and Physic 115 (2009) 313–321.
[7] M.B. Valcarce, C. Lo'pez, M. Va'zquez, The Role of Chloride, Nitrite and Carbonate Ions on Carbon Steel Passivity Studied in Simulating Concrete Pore Solutions, Journal of the Electrochemical Society (2012) 159.
[8] D.W. Hobbs, Concrete deterioration: Causes, diagnosis, and minimising risk, International Materials Reviews 46 (2001) 117–144.
[9] C.L. Page, K.W.J. Treadaway, Aspects of the electrochemistry of steel in concrete, Nature 297 (1982) 109–115.
[10] W. Morris, M. Vázquez, Corrosion of reinforced concrete exposed to marine environment, Corrosion Reviews 20 (2002) 469–508.
[11] C.L. Page, G. Sergi, Developments in cathodic protection applied to reinforced concrete, Journal of Materials in Civil Engineering 12 (2000) 8–15.
[12] C.L. Page, V.T. Ngala, M.M. Page, Corrosion inhibitors in concrete repair systems, Magazine of Concrete Research 52 (2000) 25.
[13] A.A. Sagües, H.M. Perez Duran, R.G. Powers, Corrosion Performance of Epoxy-Coated Reinforcing Steel in Marine Substructure Service, Corrosion 47 (1991) 884–893.
[14] M.M. Jalili, S. Moradian, D. Hosseinpour, The use of inorganic conversion coatings to enhance the corrosion resistance of reinforcement and the bond strength at the rebar/concrete, Construction and Building Materials 23 (2009) 233–238.
[15] W. Morris, M. Vázquez, S.R.d. Sánchez, Efficiency of coatings applied on rebars in concrete, Jounal of Materials Science 35 (2000) 1885–1890.
[16] J.M. Gaidis, Chemistry of corrosion inhibitors, Cement & Concrete Composites 26 (2004) 181.
[17] V.S. Sastri, Corrosion Inhibitors. Principles and Applications, John Wiley & Sons, West Sussex, England, 1998.
[18] T.A. Söylev, M.G. Richardson, Corrosion inhibitors for steel in concrete: state of the art report, Construction and Building Materials 22 (2008) 609.

[19] M.B. Valcarce, M. Vazquez, Carbon steel passivity examined in alkaline solutions: the effect of chloride and nitrite ions, Electrochimica Acta 53 (2008) 5007.
[20] C.M. Hansson, L. Mammoliti, B.B. Hope, Corrosion inhibitors in concrete. Part I: the principles, Cement & Concrete Composites 28 (1998) 1775–1781.
[21] S.M. Abd El Haleem, S. Abd El Wanees, E.E. Abd El Aal, A. Diab, Environmental factors affecting the corrosion behavior of reinforcing steel. IV. Variation in the pitting corrosion current in relation to the concentration of the aggressive and the inhibitive anions, Corrosion Science 52 (2010) 1675–1683.
[22] Y.B. Gao, J. Hu, J. Zuo, Q. Liu, H. Zhang, S.G. Dong, R.G. Du, C.J. Lin, Synergistic inhibition effect of sodium tungstate and hexamethylene tetramine on reinforcing steel corrosion, Journal of the Electrochemical Society 162 (2015) C555–C562.
[23] Y. Tang, G. Zhang, Y. Zuo, The inhibition effects of several inhibitors on rebar in acidified concrete pore solution, Construction and Building Materials 28 (2012) 327–332.
[24] N. Etteyeb, M. Sanchez, L. Dhouibi, C. Alonso, C. Andrade, E. Triki, Corrosion protection of steel reinforcement by a pretreatment in phosphate solutions: Assessment of passivity by electrochemical techniques, Corrosion Engineering Science and Technology 41 (2006) 336–341.
[25] J.M.R. Génin, L. Dhouibi, P. Refait, M. Abdelmoula, E. Triki, Influence of phosphate on corrosion products of iron in chloride-polluted-concrete-simulating solutions: Ferrihydrite vs green rust, Corrosion 58 (2002) 467–478.
[26] D.M. Bastidas, M. Criado, S. Fajardo, A. La Iglesia, J.M. Bastidas, Corrosion inhibition mechanism of phosphates for early-age reinforced mortar in the presence of chlorides, Cement and Concrete Composites 61 (2015) 1–6.
[27] N. Etteyeb, L. Dhouibi, H. Takenouti, M.C. Alonso, E. Triki, Corrosion inhibition of carbon steel in alkaline chloride media by Na_3PO_4, Electrochimica Acta 52 (2007) 7506–7512.
[28] M. Reffass, R. Sabot, M. Jeannin, C. Berziou, P. Refait, Effects of phosphate species on localised corrosion of steel in NaHCO3 + NaCl electrolytes, Electrochimica Acta 54 (2009) 4389–4396.
[29] L. Yohai, M. Vázquez, M.B. Valcarce, Phosphate ions as corrosion inhibitors for reinforcement steel inchloride-rich environments, Electrochimica Acta 102 (2013) 88–96.
[30] H. Nahali, L. Dhouibi, H. Idrissi, Effect of phosphate based inhibitor on the threshold chloride to initiate steel corrosion in saturated hydroxide solution, Construction and Building Materials 50 (2014) 87–94.
[31] L. Dhouibi, E. Triki, M. Salta, P. Rodrigues, A. Raharinaivo, Studies on corrosion inhibition of steel reinforcement by phosphate and nitrite, Materials and Structures/Materiaux et Constructions 36 (2003) 530–540.
[32] J.J. Shi, W. Sun, Effects of phosphate on the chloride-induced corrosion behavior of reinforcing steel in mortars, Cement & Concrete Composites 45 (2014) 166–175.
[33] B. Elsener, Corrosion inhibitors for steel in concrete. State of the art report, Maney Publishing, London, 2001.
[34] N. Etteyeb, M. Sánchez, L. Dhouibi, M.C. Alonso, H. Takenouti, E. Triki, Effectiveness of pretreatment method to hinder rebar corrosion in concrete, Corrosion Engineering, Science and Technology 45 (2010) 435–441.
[35] C. Andrade, S. Alonso, M. Acha, B. Malric, Preliminary testing of Na_2PO_3F as curative corrosion inhibitor for steel reinforcements in concrete, Cement and Concrete Research 22 (1992) 869–881.
[36] H. Nahali, L. Dhouibi, H. Idrissi, Effect of Na_3PO_4 addition in mortar on steel reinforcement corrosion behavior in 3% NaCl solution, Construction and Building Materials. 78 (2015) 92–101.
[37] D.M. Bastidas, M. Criado, V.M. La Iglesia, S. Fajardo, A. La Iglesia, J.M. Bastidas, Comparative study of three sodium phosphates as corrosion inhibitors for steel reinforcements, Cement & Concrete Composites 43 (2013) 31–38.
[38] L. Yohai, W. Schreiner, M. Vázquez, M.B. Valcarce, Phosphate ions as effective inhibitors for carbon steel in carbonated solutions contaminated with chloride ions, Electrochim. Acta 202 (2016) 231–242.
[39] ZPlot for Windows Scribner Associates Inc.1998.
[40] C. Monticelli, A. Frignani, G. Trabanelli, A study on corrosion inhibitors for concrete application, Cement and Concrete Research 30 (2000) 635.
[41] J. Wei, J.H. Dong, W. Ke, EIS study on corrosion evolution of chemical quenched rebar in concrete contaminated with chloride, Corrosion Engineering, Science and Technology 47 (2012) 31–37.
[42] J.A. González, J.M. Miranda, N. Birbilis, S. Feliu, Electrochemical techniques for studying corrosion of reinforcing steel: limitations and advantages, Corrosion 61 (2005) 37–50.
[43] W. Morris, A. Vico, M. Vazquez, S.R.d. Sanchez, Corrosion of reinforcing steel evaluated by means of concrete resistivity measurements, Corrosion Science 44 (2002) 81–99.
[44] O.A. Hodhod, H.I. Ahmed, Modeling the service life of slag concrete exposed to chlorides, Ain Shams Engineering Journal 5 (2014) 49–54.